13,18

Graphene-based biosensor: Biomolecules coupling in the de Jannes and Fröhlich models

© S.Yu. Davydov

Ioffe Institute,
St. Petersburg, Russia

E-mail: Sergei_Davydov@mail.ru

Received April 25, 2024
Revised April 25, 2024
Accepted June 15, 2024

A three-layer structure consisting of epitaxial graphene and two organic macromolecules: a biore-ceptor (antibody) deposited on graphene and a biomarker (antigen) in contact with it. Simple analytical estimates of antigen adhesion to antibody made within the framework of the de Gennes and Fröhlich models are presented. Numerical estimates have shown that the main mechanism for coupling of biomolecules is their stitching by monomeric macromolecule connector (de Jannes model).

Keywords: graphene, antibody (bioreceptor), antigen (biomarker), stitching by monomers.

DOI: 10.61011/PSS.2024.08.59066.91

1. Introduction

The research interest in development of resistive graphene biosensors suitable for rapid medical diagnostics has been on the rise lately [1–8]. The structure of such a biosensor is shown schematically in Figure 1. In the initial state, the sensor contains single-sheet graphene formed on a semiconductor substrate (for example, SiC polytype) with an antibody Ab (bioreceptor), which is an organic macromolecule (MM), on its surface [7]. In the process of measurement, the tested biomolecule (antigen Ag, biomarker) is brought into contact with Ab [7,8]. The interaction of Ag with Ab alters the conductivity of encapsulated graphene, which is detected by the biosensor and serves as an indicator of the presence of an antigen. Sufficiently strong antibody–graphene and antigen–antibody bonds are needed for stable biosensor operation. The present study is focused on evaluating the strength of the latter bond.

From a theoretical standpoint, the complexity of this task stems from the structure of biomolecules, which have the shape of plaques formed, e. g., by beta-amyloid peptide ($A\beta$) with a molecular mass of $4 \cdot 10^3$ hydrogen masses and a length of about 40 amino-acid residues (one unstructured amino-acid residue is 0.36 nm in length). In addition, the geometry of such a plaque and the area of its contact with the substrate or a plaque of another biomolecule are both unknown and variable quantities. Therefore, DFT cannot be applied directly in this case. At the same time, there is no doubt that radically simplified approaches are needed to compile a model description of the MM–substrate system. Therefore, an extremely simple dangling bonds model (DBM) was proposed in [9] for the interaction of bioreceptor Ab with graphene. Dangling bonds are understood as the bonds of MM (i. e., biomolecule Ab) fragments bordering on graphene with energies ε_i and concentrations $N_i = m_i/S$, where m_i is the number of dangling bonds of type i in a unit cell of graphene with area $S = \frac{3\sqrt{3}}{2} a^2$, where a is the distance between the nearest neighbors in graphene. This approach provided an opportunity to obtain analytical expressions for adhesion energy E_{adh} of MM on graphene, which is (according to rough estimates) on the order of several J/m^2. Two simple models of coupling of Ab and Ag biomolecules are presented below.

2. De Gennes model

Let us start the examination of the antibody–antigen interaction by reviewing the de Gennes model proposed in jcite10,11. These studies were published after the experimental demonstration of the fact that adhesion energy E_{adh} of two layers of rubber is $10^2 - 10^3$ J/m^2, whereas the corresponding van der Waals adhesion is 4–5 orders of magnitude weaker [12]. De Gennes suggested that large E_{adh} values are the result of stitching of two MMs by organic contactor monomers crossing the space between MMs

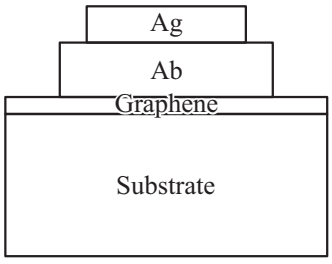

Figure 1. Graphene-based biosensor diagram. Ab–antibody (bioreceptor macromolecule); Ag–antigen (biomarker macromolecule). The current flows along the graphene sheet.

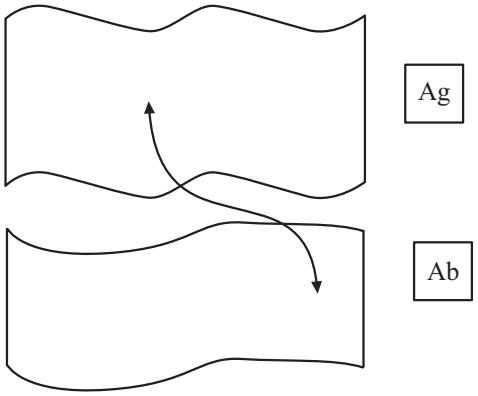

Figure 2. Diagram of stitching of fragments of Ag and Ab biomolecules by a monomer connector. Its section corresponding to one stitch is represented by a line with arrows.

(gap) and penetrating into their inner regions (Figure 2). A contactor may cross the gap not just once (as in Figure 2), but multiple times (see [10,11]). It was assumed that contactors are formed from the same atoms as MMs. The theory of elasticity and thermodynamics of solutions were used to estimate the value of E_{adh}. Here, we take into account only the fact that the coupling of two MMs gets disrupted when the contactor monomer is ruptured in the gap area.

According to [13], energyE_b of the diatomic σ-bond in the Harrison theory [14,15] is

$$E_b = -\frac{2V_2}{\alpha_c}\left(1 - \frac{2}{3}\alpha_c^2\right). \qquad (1)$$

Here, $V_2 = -3.19\hbar^2/(ma^2)$ is the covalent energy of the $sp\sigma$-bond of atoms A and B ($\hbar$ is the reduced Planck constant, m is the mass of a free electron, and a is the distance between nearest neighbors); $\alpha_c = V_2/\sqrt{V_2^2 + V_3^2}$ is the bond covalence, $V_3 = |\varepsilon_{sp}^{\text{A}} - \varepsilon_{sp}^{\text{B}}|/2$ is the polar energy for the $sp\sigma$-bond of atoms A and B, and $\varepsilon_{sp}^{\text{A(B)}} = (\varepsilon_s^{\text{A(B)}} + \varepsilon_p^{\text{A(B)}})/2$ [16]. The values of terms of the s and p states $\varepsilon_{s(p)}$ are given in [15]. Assuming that a is equal to the sum of atomic radii $r_a^{\text{A}} + r_a^{\text{B}}$, which were given in [17], we find the values of E_b presented in the table.

The choice of fragments is consistent with the estimates made in [9]. It follows from the table that $E_b \approx 2V_2/3$ for the chosen fragments, and the approximate equality turns into an exact one in the case of dimers with A = B. The obtained estimates correspond to fragments located inside the gap (i. e., at $a < h$).

Characteristics of probable diatomic fragments of the connector monomer

Connector fragment	a, Å	V_2, eV	V_3, eV	α_c	E_b, eV
CN	1.48	11.1	2.39	0.98	8.1
CO	1.51	10.7	5.08	0.90	10.9
NO	1.45	11.6	2.70	0.97	8.9

Assuming that area $S^* = 1\,\text{nm}^2$ of the Ab–Ag contact corresponds to a single connector crossing the gap, we obtain $E_{\text{adh}} \approx 1\,\text{J/m}^2$ (i. e., a value of the same order of magnitude as the one found for Ab adhesion on graphene [9]). Unfortunately, we have no knowledge on the values of S^*.

3. Fröhlich model

Static Ab–Ag coupling was considered above. Following the Fröhlich model [18], we now examine two MMs with linear dimensions L located at distance $R \gg L$ from each other and having the firm of giant dipole moments $\mathbf{p}_1$ and $\mathbf{p}_2$ oscillating with frequencies ω_1 and ω_2 (in the present case, the term „MM fragments“ is more fitting). If interaction is enabled between these MMs, the system will be characterized by frequencies

$$\omega_{1,2}^2 = \frac{1}{2}(\omega_1^2 + \omega_2^2) \pm \left[\frac{1}{4}(\omega_1^2 - \omega_2^2)^2 + \frac{\beta^2}{\varepsilon_\pm^2}\right]^{1/2}, \qquad (2)$$

where $\varepsilon_\pm$ is the permittivity of the gap at frequencies $\omega\pm$ and parameter β corresponds to the MM interaction. If MM1(2) contains $N_{1(2)}$ particles with mass m and charge e, $\beta^2 \approx e^4 N_1 N_2/(m^2 R^6)$. A more thorough analysis [19] revealed that interaction energy $U(R)$ of macromolecules 1 and 2 at $\omega_1 \gg \omega_2$ or $\omega_2 \gg \omega_1$ (i. e., out of resonance) in the $r \ll c/\omega_{1,2}$ limit (near region), where c is the speed of light, is given by $U(R) \propto \pm|\chi'(R, \omega_{1,2})|^2 \cong \pm 1/R^6$ (short-range action) [19], where $\chi'(R, \omega)$ is the real part of susceptibility of the system. The obtained expression for $U(R)$ matches van der Waals energy $U_{\text{vdW}}(R)$, but differs from it in nature, since true $U_{\text{vdW}}(R)$ is associated with the exchange of virtual photons between macromolecules, whereas the present case involves actual exchange of electromagnetic energy. At $r \gg c/\omega_{1,2}$ (far region), we obtain oscillating interaction with an envelope decreasing as R^{-2} (long-range action) [19]. In the case of $\omega_1 \approx \omega_2 = \omega_0$ (resonant region), we find $U(R) \propto R^{-\alpha}$, where $\alpha \leq 3$. Thus, the electromagnetic interaction between identically oscillating dipoles is long-range in nature. In the $r \ll c/\omega_{1,2}$ limit (near region), we obtain $U(R) \propto \pm|\chi'(R, \omega_{1,2})|^2 \approx \pm 1/R^3$ [19]. In the intermediate and far regions, the interaction is oscillating with an envelope proportional to R^{-1}. According to the estimates presented in [19], $E_{\text{adh}} \sim |U(R)|/S^* \sim 4 \cdot 10^{-3}\,\text{J/m}^2$ in the case of resonance at $T = 300\,\text{K}$, $\varepsilon_+ \approx \varepsilon_- = \varepsilon_0 = 1$, and $R = 10\,\text{nm}$. Thus, in terms of adhesion, the primary Ab–Ag coupling mechanism is stitching with MM organic connectors.

4. Conclusion

Thus, it was demonstrated that the de Gennes adhesion of Ag on Ab is far stronger than the Fröhlich adhesion and reaches a level of $1\,J/m^2$, which is consistent in order of magnitude with the adhesion of Ab on graphene [9]. Note that the difficulty of estimating $E_{adh} = V_b/S^*$ stems primarily from the uncertainty of S^*.

As for the biosensor operation, one major difference between the de Gennes and Fröhlich models should be noted. If a monomer connector penetrates an antibody and is bound to graphene, this binding corresponds to the emergence of a new scattering center. The mobility of carriers in graphene should decrease as a result [21], and this again brings up the question of the S^* value, which specifies the concentration of scattering centers induced by the connector.

Funding

This study was supported by grant 22-12-00134 from the Russian Science Foundation.

Conflict of interest

The author declares that he has no conflict of interest.

References

[1] Y. Bai, T. Xu, X. Zhang. Micromachines **11**, *1*, 60 (2020).
[2] M. Coroş, S. Pruneanu, R.-I. Stefan-van Staden. J. Electrochem. Soc. **167**, *3*, 037528 (2020).
[3] V. Naresh, N. Lee. Sensors **21**, *4*, 1109 (2021).
[4] S. Shahriari, M. Sastry, S. Panjikar, R.K. Singh Raman. Nanotechnol. Sci. Appl. **14**, 197 (2021).
[5] Laxmi, B. Mahapatra, R.V. Krishna, P.K. Patel. AIP Conf. Proc. **2327**, *1*, 020011 (2021).
[6] A.A. Lebedev, S.Yu. Davydov, I.A. Eliseyev, A.D. Roenkov, O. Avdeev, S.P. Lebedev, Y. Makarov, M. Puzyk, S. Klotchenko, A.S. Usikov. Mater. **14**, *3*, 590 (2021).
[7] S.V. Vorob'ev, S.N. Yanishevskii, A.Yu. Emelin, A.A. Lebedev, S.P. Lebedev, Yu.N. Makarov, A.S. Usikov, S.A. Klotchenko, A.V. Vasin. Klin. Lab. Diagn. **67**, *1*, 5 (2022). (in Russian).
[8] S. Wang, X. Qi, D. Hao, R. Moro, Y. Ma, L. Ma. J. Electrochem. Soc. **169**, *2*, 027509 (2022).
[9] S.Yu. Davydov. Phys. Solid State **64**, *12*, 2018 (2022).
[10] E. Raphael, P.G. de Gennes. J. Phys. Chem. **96**, *10*, 4002 (1992).
[11] H. Ji, P.-G. de Gennes. Macromolecules **26**, *3*, 520 (1993).
[12] H.R. Brown. Macromolecules **24**, *10*, 2752 (1991).
[13] S.Yu. Davydov, O.V. Posrednik. Phys. Solid State **57**, *4*, 837 (2015).
[14] W.A. Harrison. Phys. Rev. B **27**, *6*, 3592 (1982).
[15] W.A. Harrison. Phys. Rev. B **31**, *4*, 2121 (1985).
[16] S.Yu. Davydov, G.I. Sabirova. Tech. Phys. Lett. **57**, *6*, 515 (2011).
[17] Fizicheskie velichiny. Spravochnik / Ed. by E.S. Grigor'ev, E.Z. Meilikhov. Energoatomizdat, M. (1991). (in Russian).
[18] H. Fröhlich. Adv. Electronics. Electron. Phys. **53**, 85 (1980).
[19] J.R. Reimers, L.K. McKemmish, R.H. McKenzie, A.E. Mark, N.S. Hush. PNAS **106**, *11*, 4219 (2009).
[20] J. Preto, M. Pettini, J.A. Tuszynski. Phys. Rev. E **91**, *5*, 052710 (2015).
[21] S.Yu. Davydov, A.A. Lebedev, Semiconductors **57**, *5*, 395 (2023).

Translated by D.Safin